УДК 539.1.074.55, 539.184.3

IS THE THERMAL-SPIKE MODEL CONSISTENT WITH EXPERIMENTALLY DETERMINED ELECTRON TEMPERATURE?

E.A. Ayrjan, A.V. Fedorov, B.F. Kostenko

Carbon K-Auger electron spectra from amorphous carbon foils induced by fast heavy ions are theoretically investigated. The high-energy tail of the Auger structure showing a clear projectile charge dependence is analyzed within the thermal-spike model framework as well as in the frame of another model taking into account some kinetic features of the process. A poor comparison results between theoretically and experimentally determined temperatures are suggested to be due to an improper account of double electron excitations or due to shake-up processes which leave the system in a more energetic initial state than a statically screened core hole.

The investigation has been performed at the Laboratory of Computing Techniques and Automation, JINR.

Согласуется ли модель температурного пика с экспериментально определенной температурой электронов?

Э.А.Айрян, А.В.Федоров, Б.Ф.Костенко

Изучаются спектры Оже-электронов, испущенных из аморфного углерода под воздействием ускоренных ионов. Высокоэнергетичные хвосты Оже-структуры, зависящие от заряда налетающей частицы, проанализированы в рамках модели температурного пика, а также в рамках другой модели, учитывающей некоторые кинетические особенности процесса. Плохое согласие теории и эксперимента объясняется не вполне удовлетворительным расчетом двойных электронных возмущений,неучетом процессов встряхивания, переводящих систему в более энергетичное начальное состояние по сравнению с тем, что дает модель статически заэкранированной дырки на K-оболочке.

Работа выполнена в Лаборатории вычислительной техники и автоматизации ОИЯИ.

1. INTRODUCTION

At present transient thermal models taking into account the electron and phonon degrees of freedom are successfully used for explanation of track formation in thin films and small grains of pure materials as well as for description of phase transitions of surfaces after

femtosecond laser irradiation (see, e.g., [1–5] and references therein). A growing interest to such problems is stimulated now by the problem of atomic energy production on the basis of a particle accelerator hybrid together with a uranium or thorium target reactor [6].

Therefore, it was rather unexpected that the first experimental results on electron temperatures in the center of the nuclear track showed a serious disagreement with calculations of electron temperature in the framework of the thermal-spike model [7]. In this model the space and time evolution of electron and atom systems are governed by a set of coupled nonlinear differential equations [1,8]

$$\rho C_e(T_e)\frac{\partial T_e}{\partial t} = \frac{\partial}{\partial r}\left[K_e(T_e)\frac{\partial T_e}{\partial r}\right] + \frac{K_e(T_e)}{r}\frac{\partial T_e}{\partial r} - g(T_e - T_i) + A(r,t), \tag{1}$$

$$\rho C_i(T_i)\frac{\partial T_i}{\partial t} = \frac{\partial}{\partial r}\left[K_i(T_i)\frac{\partial T_i}{\partial r}\right] + \frac{K_i(T_i)}{r}\frac{\partial T_i}{\partial r} + g(T_e - T_i),$$

where T_e and T_i are electrons and lattice temperatures, respectively, C_e, C_i and K_e, K_i being the specific heat and thermal conductivity for the electronic system and lattice, ρ is the material density, g is the electron-atom coupling, $A(r,t)$ is the power brought on the electronic system in a time considerably less than the electronic thermalization time, and r stands for the radius in cylindrical geometry with the ion path as the axis. According to paper [7], theoretical predictions turned out to be about a factor five lower than the experimental values.

It should be noted that the observed temperatures, being of order of several eV, have been deduced from an analysis of electron spectrum within the range 260–300 eV. Therefore, there is a big danger to overestimate the experimental temperatures if not exclude the fast δ-electrons properly. It seems plausible, however, that the authors are quite aware of such a problem (see [9]). Since even the maximum electron temperature — which is maintained during a short time when cooling due to thermal diffusion is negligible — in thermal-spike model is smaller than observed one [7], there is a need to revise first of all calculations of the dynamics of radial energy deposition in the vicinity of ion trajectory together with reconsideration of the used estimate for the electron specific heat.

2. THE ENERGY DENSITY PER UNIT TIME AND THE ELECTRONIC SPECIFIC HEAT

The time dependent radial distribution of dose from delta-rays about the ions path in this paper was calculated in line with [10, 11]. This approach takes into account the dynamics of energy deposition in more detailed form then it was done in [8]. In the first approximation, the δ-electrons trajectories are considered to be perpendicular to the ion one, so that the time of electron arrival to a point at a distance b from the centre of ion path is equal to

$$t(b) = \int_0^b \frac{db}{v(b)} = \int_{R-b}^{R} \frac{dr}{v(R-r)} = \frac{1}{c}\int_{E(R-b)}^{E(R)} dE\left(\frac{dr}{dE}\right)\frac{E+mc^2}{[E(E+2mc^2)]^{1/2}}, \tag{2}$$

$r = r(E)$ being the range-energy relation for electrons in a-C, c is the speed of light, m is the electron mass. To account for small angle scattering important in the region $b = 1 - 10$ nm,

some corrections to this picture were also included [10, 11]. The energy deposition at moment t in volume $2\pi\ b\ db\ \times$ unit pathlength is determined by

$$\varepsilon(b,t) = \frac{1}{2\pi b}\int_{E(b,t)}^{E_max}\left(-\frac{dE(R-b)}{db}\right)\frac{dN}{dE}dE,$$

where $E(b,t)$ is the solution of equation (2), dN/dE stands for the number of delta-rays per energy unit which is calculated using the Rutherford formula. The range-energy relation $r(E)$ and its inverse $E(r)$ were approximated from known experimental and theoretical data and comparison of the model with experimental stopping power shows 10% accuracy in a wide range of energies and projectile nuclei. The energy deposition in the first 10 $\mathring{A}$ which is the most important in the context of the problem under consideration was taken strictly in accordance with [10]. In particular, we obtain the dose $7\cdot 10^4\ \ J/\mathrm{cm}^3$ at $b = 1\ \mathring{A}$.

Now, let us turn to calculation of the electronic specific heat. The electronic density of states (DOS) in a-C resulted from the molecular-dynamics computation [12] is displayed in Fig. 1 by a solid line stretching from -20 to 10 eV.

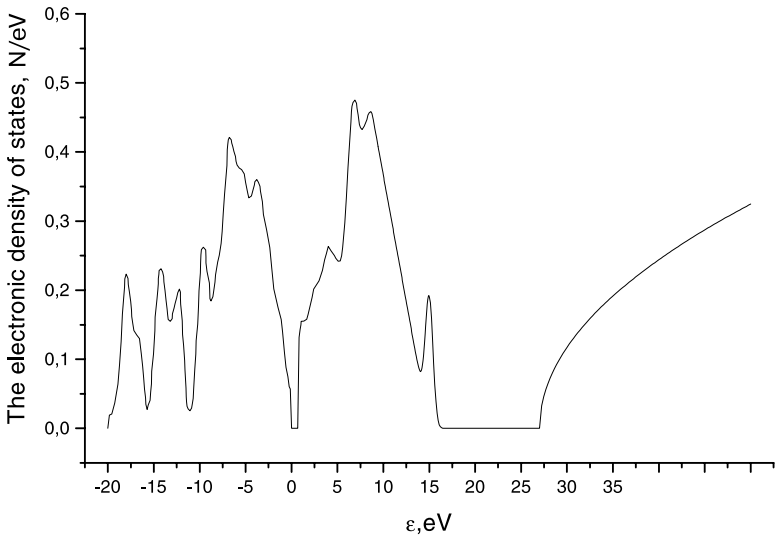

Fig. 1. The electronic density of states in a-C (explanation in the text)

Normalizing factor of the curve $D(\varepsilon)$ stems from an obvious condition

$$\int_{-20}^{0} D(\varepsilon)d\varepsilon = 4,$$

which means that the valence band contains at low temperatures four electrons per atom. To estimate the role of highly excited states of the conduction band, we extended the calculated curve from 10 to 20 eV so that

$$\int_{-20}^{0} D(\varepsilon)d\varepsilon = \int_{0}^{20} D(\varepsilon)d\varepsilon.$$

The last condition follows from the existence of nearest-neighbor or, even, medium-range order in a-C , which produces some of the characteristic features of the single-crystal DOS [13]. Though the precise behaviour of the DOS in the region $10 < \varepsilon < 20$ eV is unknown, one has to bear in mind that a contribution of those states to observable quantities is exponentially suppressed at temperatures $k_B T < 10$ eV. We also take into account a small experimentally observed gap of about 0.4 – 0.9 eV existing between valence and conduction bands [14]. The gap between valence band and continuum resulting from a condition of the electron refraction at the surface of evaporated carbon is taken to be about 27 eV [15]. Finally, DOS for continuum can be evaluated in the quasi-classical approximation [16],

$$D(\varepsilon) = v\frac{\sqrt{2}m^{3/2}}{\pi^2\hbar^3}\sqrt{\varepsilon - 27},$$

where v is the spatial volume per atom, $v = 0.9963\ 10^{-23}\text{cm}^3$ for $\rho = 2$ g cm^{-3}.

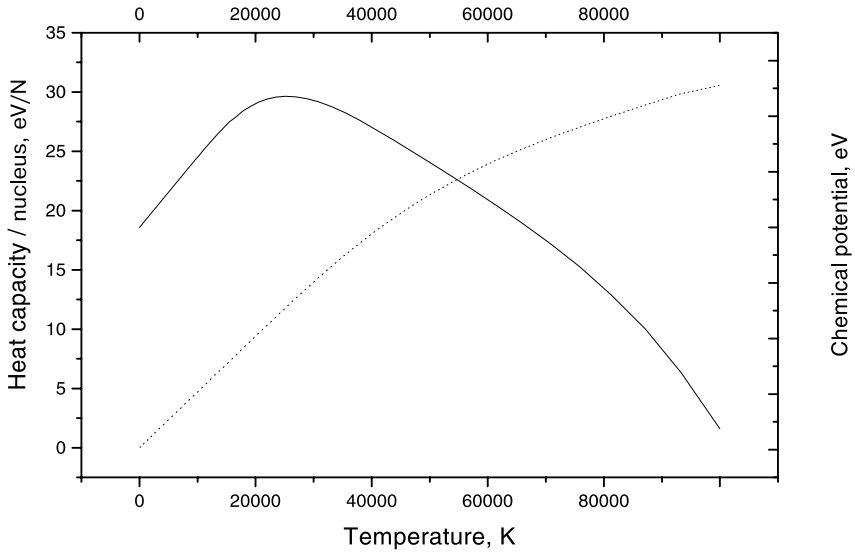

Fig. 2. The chemical potential $\mu(T)$ and the specific heat per atom C_V (solid and dotted lines, respectively)

Considering electrons in a-C as a perfect gas, we have for its energy:

$$E = \int_{-20}^{0}(-\varepsilon)(1 - f(\varepsilon, T))dn(\varepsilon) + \int_{0}^{\infty}\varepsilon f(\varepsilon, T))dn(\varepsilon), \tag{3}$$

where $f(\varepsilon, T)$ is the Fermi distribution, and $dn(\varepsilon) = D(\varepsilon)d\varepsilon$. The chemical potential $\mu(T)$ is determined in a usual way by the equation of conservation of the number of particles:

$$\int_{-20}^{\infty} f(\varepsilon, T)dn(\varepsilon) = 4.$$

The solution of it, as well as other calculations in this paper, was obtained within mathematical environment of MAPLE and is represented by the solid line in Fig. 2.

The specific heat per atom can be found by direct differentiation of relation (3),

$$C_V = \frac{dE}{dT} = \int_{-20}^{\infty} \varepsilon \, \frac{f(\varepsilon, T)}{dT} dn(\varepsilon),$$

and is shown in Fig. 2 by the dotted line.

3. CALCULATIONS AND THEIR INFERENCES

Using electronic specific heat and the radial energy deposition described above, we performed the thermal-spike calculations of the radial electron temperature distribution as a function of the time. A program which had been written first to describe the thermal relaxation processes in high T_c superconductors [17], after appropriate physical and mathematical alterations, was adapted for this purpose.

Estimations of the electron temperature T_e in the vicinity of ion trajectory contain uncertainties unrecognizable at sight. For example, one has to fix in a reasonable way a volume in which the mean value of temperature is determined. It is also important to control a time, when the temperature is reached. If this time is less than the characteristic Auger decay time in a-C, $\tau_A \sim 10^{-14}$ s, then it is clear that calculated T_e has nothing to do with a real electron temperature, since the model does not incorporate a contribution of the atom core into description. Here we assume a simple model of "registration" which takes into account all these factors.

The number of electrons emitted from the surface into a direction of registration is

$$N(\varepsilon) = \frac{d\Omega}{4\pi} \int_{r_{\min}}^{\infty} 2\pi r \, dr \int_{t_{\min}}^{\infty} dt \, j(\varepsilon, T),$$

where $j(\varepsilon, T) = D(\varepsilon) f(\varepsilon, T) v(\varepsilon)$ stands for the density of current, and $d\Omega$ denotes the spherical sector of registration. Parameters $r_{\min}$, $t_{\min}$ were estimated from physical reasons of applicability of the model and were chosen to be

$$r_{\min} \simeq 10^{-8} \text{ cm}, \qquad t_{\min} \simeq 10^{-15} s.$$

The temperature $T = T(r, t)$ was determined by the equations (1) with the thermal diffusivity of electrons $D_e = K_e/C_e \simeq 1/20$ cm^{2}s^{-1}. We assume that the experimentally registered temperature T_e corresponds to the theoretical value determined as the solution of equation

$$\exp(-\Delta\varepsilon / k_B T_e) = N(\varepsilon + \Delta\varepsilon)/N(\varepsilon),$$

where ε and $\varepsilon + \Delta\varepsilon$ belong to the interval of registration. Though an essential part of dose is deposed after moment $t_{\min}$, we found that the energy distribution $N(\varepsilon)$ is determined mainly by its form at $t_{\min}$,

$$N(\varepsilon) \simeq C(t_{\min}) J(t_{\min}, \varepsilon),$$

with $J = 2\pi \int j \; r \; dr$. At the same time the electron temperature proves to be practically independent of the further decrease of $r_{\min}$. The result of calculations is depicted in Fig. 3.

We see that despite of the undertaken improvements our results confirm the conclusion that the thermal-spike model predicts electron temperatures which are about a factor 1.5 lower

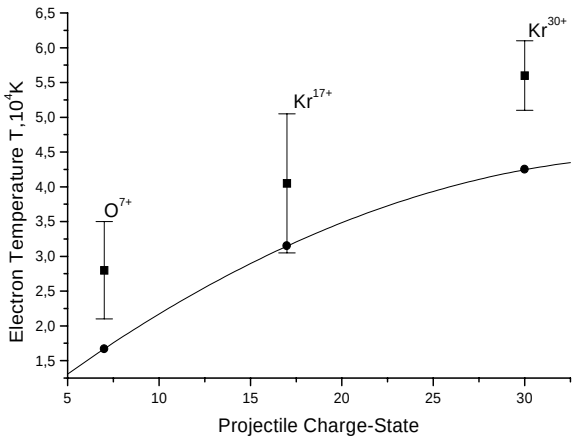

Fig. 3. Electron temperature in amorphous carbon as a function of the initial projectile charge (O^{7+}, Kr^{17+}, Kr^{30+}) at projectile energy of 5 MeV/u in comparison with the results of the thermal-spike model

than ones determined in [7]. It is impossible to achieve a better agreement from accounting for final-state hole-hole repulsion (this interaction could only reduce the theoretical yield of hot electrons). It is obvious that the existing uncertainties in the thermal conductivity of electrons do not influence significantly the theoretical temperatures because of smallness of electron emission time into registered part of spectrum.

The resume of these considerations is that the thermal-spike model is inapplicable to the description of the experimental data obtained in [7]. In our opinion such conclusion is natural and was predictable beforehand. Indeed it is well-known that the electrons detected in [7] after subtraction of a continuous background of δ-electrons consist primarily of Auger electrons which have suffered inelastic energy losses in the material [9]. A theory of these processes is developed on the basis of abundant experimental information including data for carbon (see [12, 18] and references therein). It takes into account some kinetic features of the process (see below) not included into the thermal spike model. Such conclusion is also supported by the direct comparison of the Auger decay time τ_A with the duration of electron emission into registered part of spectrum shown in Fig. 4.

We see that energy deposition in the region $b < 10$ nm which gives the main contribution to the observed temperature tails is finished at a time $\tau_1 \sim 10^{-15}$s, which is shorter than τ_A. Therefore, observable electrons result from decay of a nonequilibrium state which precedes a situation discribed by the thermal spike model.

4. AUGER ELECTRON SPECTRUM

Description of Auger electron ejection from a-C is subdivided in Ref. 7 into three subsequent steps:

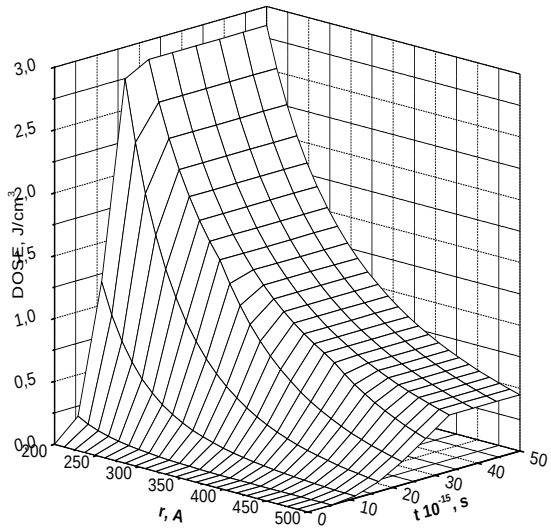

Fig. 4. The time dependence of radial distribution on the delta-ray dose around the path of O^{7+} at 5 MeV/u in a-C foil

1) initial electron production determined by Auger rates calculated at a given electron temperature T_e in the valence band,

2) transport of electrons to the surface, under the influence of elastic and inelastic collisions; particularly plasmon energy losses [12] are taken into account,

3) transmission through the surface potential described by the formula

$$F^{\text{vacuum}} = F^{\text{bulk}}(E)\frac{E}{E+V_s},$$

where $V_s \simeq 27$ eV.

Let us concentrate on the first step of the model on the ground that the contribution of the valence band temperature into observable spectrum takes place only on this stage. Energy distribution of electrons ejected due to the Auger transitions is described by the relation:

$$F(E) \sim \sum_{XY} \mid V_{XY} \mid^2 \int d\varepsilon \; n_X(\varepsilon, T_e) \; n_Y(E-\varepsilon, T_e), \tag{4}$$

where $n_X(\varepsilon, T_e) = D_X(\varepsilon) f(\varepsilon, T_e)$, $D_X(\varepsilon)$ is the density of states in a band X, $f(\varepsilon, T_e)$ is the Fermi distribution, and V_{XY} stands for the Auger matrix elements dependent on the bands, X and Y, involved. According to [12, 18] we represent DOS in the valence band as a sum of three components,

$$D(\varepsilon) = \sigma_s(\varepsilon) + \sigma_p(\varepsilon) + \pi_p(\varepsilon),$$

and take for the matrix elements ratios:

$$\mid V_{ss} \mid^2 : \mid V_{sp} \mid^2 : \mid V_{pp} \mid^2 = \; 0.8 \; : \; 0.5 \; : \; 1.0.$$

The kinetic energy of the ejected Auger electrons is approximated by the formula

$$E = I_c - I_1 - I_2 - U_h, \tag{5}$$

where $I_c = 284.6$ eV is the electron binding energy of the core, I_1 and I_2 are those of the valence levels, and U_h is effective hole-hole interaction dependent on the bands involved:

$$U_h(\sigma,\sigma) = 2 \text{ eV}, \qquad U_h(\sigma,\pi) = 1.5 \text{ eV}, \qquad U_h(\pi,\pi) = 0.6 \text{ eV}. \tag{6}$$

In contrast to [7], we also take into account the dependence of chemical potential on T_e depicted in Fig. 2. The final formula is:

$$F(E) \sim P_{ss} n_{\sigma s} * n_{\sigma s} + P_{pp}(n_{\sigma p} * n_{\sigma p} + 2n_{\sigma p} * n_{\pi p} + n_{\pi p} * n_{\pi p}) + 2P_{sp}(n_{\sigma s} * n_{\sigma p} + n_{\sigma s} * n_{\pi p}),$$

where $P_{XY} :=\mid V_{XY} \mid^2$ and $n_{\sigma s} * n_{\sigma s}$, etc., indicate the fold calculated with account of (5) and (6).

In this model, electrons excited above the Fermi level make a contribution to the energy region $E > I_c$ of the Auger spectrum. For the calculation of the temperature-dependent peak broadening one can use the previous formulae suggesting that the excited electron state in the conduction band has *p* symmetry [18]. The temperature found in such way was interpreted in [7] as the experimentally determined electron temperature in the centre of nuclear tracks. Though this model is more appropriate for the treatment of the experimental data discussed in [7], it does not take into account the energy conservation law in the explicit manner. Therefore any contradiction between the models considered above has to be resolved in favor of the thermal-spike one which is more accurate in this respect. Our calculations show that the valence band temperature extracted by this method turns out to be still higher than the value $T_e(r_{\min}, \tau_A)$ obtained in the frame of the thermal-spike model (even if one neglects the temperature decrease due to thermal conductivity of electrons). Therefore, estimates of electron temperature given in [7] look as unreasonable, especially if one remembers that an essential fraction of the energy is not contained in the valence band excitations during the time $t \leq \tau_A$.

5. SUMMARY AND DISCUSSION

When our study was about to be completed, a paper [20] devoted to the same problem was published. It was claimed there that the contradiction between the theory and experiment can be eliminated by more accurate calculation of the electron specific heat C_e (besides the energy deposition in the first $10\mathring{A}$ was found to be about 30 % higher than in the standard model). Such conclusion contradicts our calculations, though it is difficult to explain the difference as far as neither details nor the values of $C_e(T_e)$ are given in [20]. Therefore in our paper we describe the appropriate peculiarities of the model in an explicit and easily checked form.

At the same time our calculations make us seriously doubt the electron temperatures obtained in [7]. As we have seen such high temperatures could never be reached in the valence band, if our models for the energy deposition and the electronic specific heat are true.

In the light of the previous consideration it is natural to find another explanation for the experimental carbon Auger-electron spectra. Here we consider three possibilities.

A. The observed dependence of spectrum on the projectile charge is a consequence of a poor account for the δ-electron background. Indeed, in [18] a criterion for a properly corrected background of secondary electrons was formulated. According to it, the region of the corrected spectrum with energies above the Auger threshold (>284.6 eV) should be flat and at zero baseline. In other case, a proper deconvolution of the raw experimental data cannot be made. One can see that this criterion is not met for the data represented in [7].

B. There is a dynamic screening effect which can give rise to the Auger spectrum at the Fermi level. This effect can be responsible for an increase of high energy tails if one takes into account an instrumental resolution broadening of the spectra. Namely the sudden creation of a core vacancy can lead to shake-up processes which leave the system in a more energetic initial state than a statically screened core hole. This state was registered in carbon in [18] and was identified with a valence-core exciton. In this case the resultant Auger initial state contains two positive holes, one in the core level and one in a valence level, with one electron in the excitonic level. This model can hardly explain the observed dependence of spectrum on the projectile particle charge since the shake-up process is a consequence of the creation of a hole in the K level (which "nothing knows" about an ion created it). Nevertheless, this mechanism can give a constant contribution to the valence band temperatures making them much more reasonable.

C. The third physical effect important in the context of our discussion is the creation and decay of double K vacancies. In paper [20] a constant ratio of double to single K-shell ionization probabilities (of about 0.27) was suggested. Meanwhile, experimentally observed dependence of the spectrum on the projectile may be brought about by dependence of this ratio on the projectile charge.

Acknowledgements

The research described in this publication was made possible in part by Grant No.99-01-01101 from Russian Foundation for Basic Research. The authors are grateful to A.E. Volkov, V.A. Borodin of Kurchatov Institute (Moscow) and I.N. Goncharov of JINR (Dubna) for a helpful discussion.

After discussion of the contents of this article with G. Schiewietz of Hahn Meitner Institute (Berlin), we are inclined now to exclude totally the possibility of incorrect background subtraction. At the same time, it became clear that the energy deposition model, described in [10, 11], admits some further improvements for $r < 1$ nm.

References

1. Toulemonde M., Dufour C., Paumier E. — Phys. Rev., 1992-II v.B46, p.1432.
2. Meftah A., et al. — Phys. Rev., 1994-II, v.B49, p.12457.
3. Tom H.W.K., Aumiller G.D, Brito-Cruz C.H. — Phys. Rev. Lett., 1988, v.60, p.1438.
4. Fujimoto J.G. et al. — Phys. Rev. Lett., 1984, v.53, p.1837.
5. Shank C.V., Yen R., Hirlimann C. — Phys. Rev. Lett., 1983, v.51, p.900.

6. Rubbia C. — Proc. of the Second Int. Conf. on Accelerator-Driven Transmutation Technologies and Applications, Kalmar, 3–7 June 1996, p.35.
7. Schiwietz G. et al. — Nucl. Inst. and Meth., 1998, v.B146, p.131.
8. Wang Z.G. et al. — J. Phys. Condens. Matter, 1994, v.6, p.6733.
9. Schiwietz G. et al. — Phys. Rev., 1990, v.B41, p.6262.
10. Waligorski M.P.R., Hamm R.N., Katz R. — Nucl. Tracks Radiat. Meas., 1986, v.1, p.309.
11. Barashenkov V.S. — Russ. Chem. of High Energies, 1994, v.28, p.229.
12. Galli G. et al. — Phys. Rev., 1996-II, v.B42, p.7470.
13. Schäfer J. et al. — Phys. Rev., 1996-II, v.B53, p.7762.
14. Shimakava K., Miyake K. — Phys. Rev. Lett., 1988, v.61, p,994.
15. Rösler M., Brauer W. — Particle Induced Electron Emission, Springer Tracts of Mod. Phys. v.122, Springer, Berlin, 1991.
16. Landau L.D., Lifshitz E.M. — Statistical Physics, Pergamon Press, London-Paris, 1958.
17. Barashenkov V.S., Filinova V.P., Kostenko B.F. — The First Int. Conf. «Modern Trends in Computational Physics», E5,11-98-113, Dubna, 1998.
18. Houston J.I. et al. — Phys. Rev., 1986, v.B34, p.1215.
19. Attekum P.M.Th.M., Werheim G.K. — Phys. Rev. lett., 1979, v.43, p.1896.
20. Schiwietz G. et al. — Europhys. Lett., 1999, v.47, p.384.

Received December 28, 1999.